The Aerolens: An Evaluation Study based on Computational Methods and Mass Spectrometric Tests

Dimitris Papanastasiou[1]; Diamantis Kounadis[1]; Alexander Lekkas[1]; Athanasios Zacharos[2]; Ioannis Nikolos[2]; Ioannis Orfanopoulos[1]; Emmanuel Raptakis[1]

[1]Fasmatech Sci & Tech, Athens, GR; [2]Technical University of Crete, Dept of Production Engineering, Chania, GR

INTRODUCTION

Ion transport through the atmospheric pressure interface and operation of ion optical systems immersed in fast transient gas flows have received significant attention as part of a greater effort to enhance sensitivity in Mass Spectrometry (MS) instrumentation. Transformation of the supersonic jet into a subsonic fully-developed laminarized gas flow was recently demonstrated experimentally using Particle Tracking Velocimetry (PTV)[1]. The aerolens, the newly proposed ion optical device specifically designed to suppress turbulence and control ion diffusion at intermediate pressure is further explored here using ion tracing algorithms in realistic gas flows. Preliminary data obtained with the aerolens coupled to a short ion funnel incorporated in the fore vacuum region of an oTOF MS platform are presented.

PARTICLE TRACKING VELOCIMETRY

Visualization of the gas flow at the end of a 100 mm long aerolens design with 5 mm i.d. is accomplished over an extended range of pressures. The laminarized flow visualized at the exit end of the system is presented in Figure 1 for two different pressure settings. The aerolens is assembled using 2.5 mm thick PCBs with nickel/gold-plated round holes separated by 0.5 mm spacers. The PCBs include a resistor-capacitor network to distribute DC and RF voltages to affect ion motion.

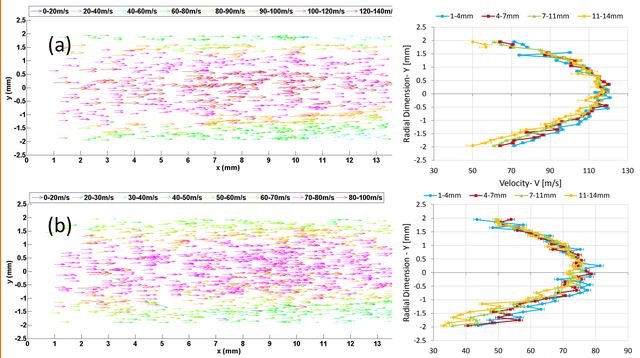

FIGURE 1. Velocity vector fields and velocity radial profiles at the exit of the PCB aerolens determined experimentally at (a) 13-20 mbar and (b) 35-50 mbar.

An expression is formulated to relate the jet pressure ratio (*JPR*) to the dimensions of the inlet aperture and those of the aerolens channel confining the jet. The cross sectional area of the channel *A* normalized to the inner cross sectional area of the inlet aperture *α* is related *JPR* through a coefficient *k* as follows:

$$\frac{A}{a} = k^2 * JPR^{1/3} \qquad [1] \qquad\qquad D = d * k * JPR^{1/6} \qquad [2]$$

The relationship for round inlet apertures and cylindrical channels is also shown. Here *D* is the diameter of the channel and *d* the diameter of the aperture or inner diameter of the inlet capillary. Effective suppression of turbulence throughout the length of the aerolens and the formation a subsonic laminarized flow is accomplished for a value of k ~8, (*D* and *d* given in mm).

ION OPTICAL SIMULATIONS

Focusing of ions was investigated in realistic gas flows using simulations. A wide range of pressures extending from 5 mbar to over 50 mbar were considered based on available PTV experimental data. DC and RF fields including their superposition are shown to provide radial compression of ions. Hard sphere collisions (SDS) code, RF potentials and experimentally determined gas flow fields were implemented through the user defined programming features available in SIMION 8.0.

Figure 2 shows ion trajectories for 150 amu ions at 5 mbar across a 100 mm long, 5 mm i.d. design with 3 mm thick electrodes and 0.5 mm spacing. Figures 1 (a) and (b) show diffusive ion motion in the absence of external electric fields under uniform gas flow conditions (100 m/s) and the PTV flow field respectively. A considerable fraction of the ions is lost on the ring electrodes. Focusing is achieved by distributing a DC potential across the rings to produce an axial profile with $\partial V^2/\partial z^2<0$. The focusing effect of such a DC gradient with 250 V applied from entrance to exit is shown in Figures 1 (c) and (d) for the uniform flow and the PTV field respectively.

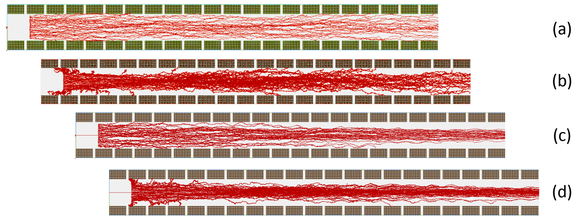

FIGURE 7. 150 amu ion trajectories in the aerolens at 5 mbar using (a) 100 m/s uniform gas flow profile and (b) the flow field determined experimental by PTV. The focusing effect of a DC gradient with $\partial V^2/\partial z^2<0$ is shown in (c) for a uniform gas flow and (d) the PTV flow field.

For the flow fields examined in Figure 1 and for ions spread uniformaly across the i.d.of the device transmission in the absence of an external electric field is ~25%. Transmission with the optimized DC gradient increases to >70%. The radial spread for ions entrained in the under-expanded jet is determined by the shear layer, thus assuming the dimensions of the aerolens entrance are chosen based on equations [1], [2] the lateral spread is considerably narrower and ion losses become negligible. Simulation results indicate that focusing becomes less effective at higher pressures and for the heavier ions. A second set of simulation results is presented in Figure 2 to demonstrate focusing in the presence of a two-phase RF field.

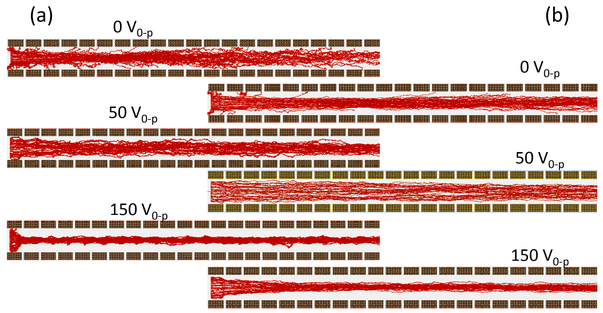

FIGURE 2. Ion trajectories at 5 mbar in the presence of a two-phase RF field at 2 MHz and different waveform amplitudes for (a) 41 amu and (b) 500 amu.

A final set of simulations is presented in Figure 3 showing the combined focusing effect of the DC gradient and the two-phase RF field at 50 mbar pressure. A 250 V DC gradient is applied toward the end of the aerolens only whilst the RF field is distributed throughout the ring electrodes and operated at 2 MHz, 250V_{o-p}. Radial compression can be accomplished for ions over 2000 amu. The focusing effect is no longer observed when the thickness of the ring electrodes was reduced to <1 mm.

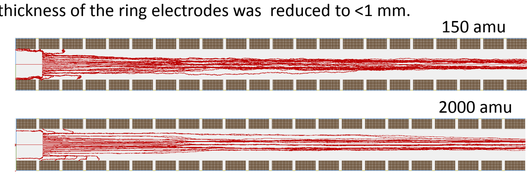

FIGURE 3. Ion trajectories at 50 mbar in the presence of a focusing DC and the two-phase RF field at 250V_{0-p}, 2 MHz.

MASS SPECTROMETRY

The aerolens is installed in the fore vacuum region of a prototype orthogonal TOF mass spectrometer equipped with an electrospray ionization source. Ions entrained in the supersonic jet are injected into the aerolens channel and radially confinement is achieved by the application of DC and RF fields, as described above. The subsonic laminar flow developed toward the distal end of the aerolens is directed into a short ion funnel. Ions are focused through a 1.6 mm pressure limiting aperture into an octapole ion guide operated at $5x10^{-3}$ - 10^{-2} mbar. A short quadrupole ion guide operated at 10^{-4} mbar transfers ions to the orthogonal TOF mass analyzer. Figure 4 (a) shows the cross section of the CAD model showing the capillary inlet with 0.5 mm i.d., the aerolens PCB device, the short funnel and the segmented octapole RF ion guide dosposed in the consecutive vacuum compartment.

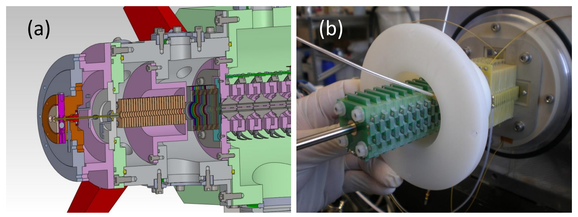

FIGURE 4. (a) CAD model cross section of the fore vacuum interface incorporating the aerolens and (b) photo showing parts during the installation.

Figure 4 (b) shows a photograph of the system with the aerolens PCB mounted on an insulating flange and positioned in front of a short ion funnel. An alignment rod is used to position the aerolens with respect to the axis of the inlet capillary. Figure 5 (a) shows the oTOF MS prototype currently operated in linear mode and 5 (b) is a typical mass spectrum obtained with a mixture of loperamide and papaverine samples at 30 nM concentration. These two molecules were used to investigate ion transmission as a function of fore vacuum pressure and a preliminary set of data is presented here.

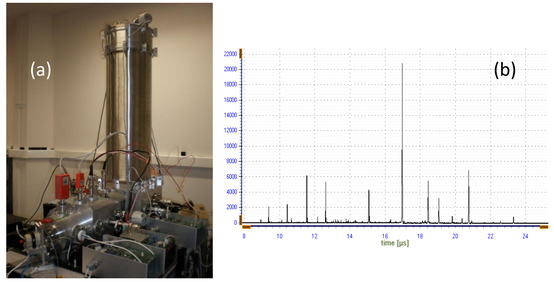

FIGURE 5. (a) photo of the oTOF MS prototype and (b) ESI mass spectrum of a 30 nM mixture of papaverine and loperamide solution in acetonitrile.

Figure 6 shows ion transmission characteristic curves as a function of pressure for (a) loperamide and (b) papaverine. Both ions exhibit a maximum around 5 mbar pressure, in contrast to solvent and source fragment ions with lower m/z values where optimum pressure can be >10 mbar. Ions are transferred with lower efficiency for the greater pressures examined up to 30 mbar.

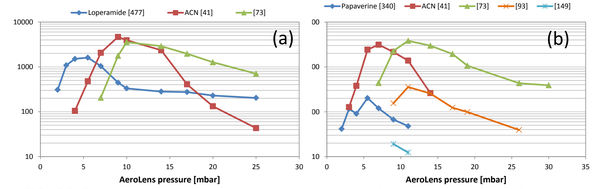

FIGURE 6. Ion transmission curves for (a) loperamide and (b) papaverine as a function of pressure.

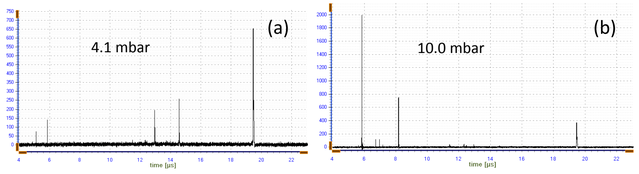

FIGURE 7. Loperamide mass spectra at (a) 4.1 mbar and (b) 10 mbar nitrogen pressure.

Figure 7 (a) shows mass spectra of loperamide obtained at 4.1 mbar and (b) 10 mbar nitrogen pressure highlighting the presence of mass discrimination effects as a function of pressure. These effects are attributed to the gas dynamical properties of the ion optical system and the application of RF potentials to the aerolens and the ion funnel. Future studies will concentrate on suppressing mass discrimination effects by optimization of the aerolens design and the gas flow presented to the funnel.

REFERENCES

Kounadis D. *et al*, A Novel Ion-Optical Design for Laminarization of Under-expanded Gas Flows, TP05, 61st ASMS Conference on Mass Spectrometry, Minneapolis, MN, 2013.